Twenty-Sixth Symposium (International) on Combustion/The Combustion Institute, 1996/pp. 1161–1169

QUANTITATIVE TWO-PHOTON LASER-INDUCED FLUORESCENCE IMAGING OF CO IN FLICKERING CH_4/AIR DIFFUSION FLAMES

DAVID A. EVEREST,[1] CHRISTOPHER R. SHADDIX[2] AND KERMIT C. SMYTH
Building and Fire Research Laboratory
National Institute of Standards and Technology
Gaithersburg, MD 20899, USA

One-dimensional fluorescence imaging measurements of CO concentrations have been made in steady and flickering axisymmetric, methane/air diffusion flames burning at atmospheric pressure. These experiments extend fluorescence detection of CO to flames that contain significant soot volume fractions, approximately 1–2 × 10^{-6}. Our aim is to quantify changes in the CO levels that occur for flickering conditions, where increased soot production and subsequent oxidation may have important effects. The Q branch (0,0) band of the $B^1\Sigma^+ \leftarrow\leftarrow X^1\Sigma^+$ transition was excited near 230 nm in a two-photon process, and the $B^1\Sigma^+ \rightarrow A^1\Pi$ (0,1) band fluorescence was detected at 483.5 nm. Quenching-independent data were obtained, and interferences from broadband molecular fluorescence and soot incandescence were accounted for by subtracting profiles measured for excitation at a nearby, nonresonant wavelength. Maximum CO concentrations are found to be approximately equal in the steady and flickering flames burning with the same fuel flow rate. For the flickering flames, the greater radial extent of the burning flamelet following clip-off yields approximately 50–65% larger volume-integrated CO levels. Overall, this increase in CO production is modest compared to the factor of 4 enhancement observed in the time-averaged, volume-integrated, soot volume fraction, indicating that soot oxidation does not appear to appreciably impact CO levels in these methane flames.

Introduction

Most detailed studies of chemical processes in diffusion flames have been carried out under steady flame conditions, which provide an environment conducive to making careful profile measurements. Flickering diffusion flames can also be investigated under reproducible experimental conditions, but in addition they exhibit time-dependent, vortex-flame-sheet interactions. Thus, flickering flames serve as an important testing ground for assessing the applicability of chemical models derived from steady flames to turbulent flows. Two examples of particular interest are the production and oxidation of soot and CO. Both involve sufficiently slow chemical rates that one might expect to observe a strong sensitivity to the complex flow fields present in time-varying flames.

Measurements of soot concentrations in steady and flickering CH_4/air diffusion flames burning with the same mean fuel flow rate have revealed a factor of 5–6 enhancement in the peak soot volume fraction and a factor of 4 increase in the time-averaged, volume-integrated soot levels for flickering flame conditions [1,2]. These higher soot levels may lead to elevated CO concentrations in the flickering flames due to several factors: (1) CO production from the oxidation of soot; CO is the primary product of soot oxidation by OH· and O_2 [3], which are the principal soot oxidizers [4]; (2) increased competition for OH· by the soot particles; high soot loadings suppress the amount of OH· available for the oxidation of CO [4]; and (3) increased radiation losses leading to lower temperatures and OH· concentrations and, thus, slower rates of CO oxidation; longer residence times available in the flickering flames [5] result in higher thermal losses than in the steady flame.

The goal of the present measurements is to quantify changes in the CO concentrations that occur in flickering diffusion flames. For the methane flames studied here, no smoke is emitted even under flickering conditions. However, for fuels that soot more heavily than methane (such as propane and ethylene), flickering flames are found to emit significant amounts of smoke at fuel flow rates that produce nonsmoking steady flames [2]. Smoke and CO emission are closely linked in both laminar and turbulent flame conditions [6,7].

[1]National Research Council NIST Postdoctoral Research Associate, 1994–1996

[2]National Research Council NIST Postdoctoral Research Associate, 1993–1995; present address: Combustion Research Facility, Sandia National Laboratories, Livermore, CA 94551

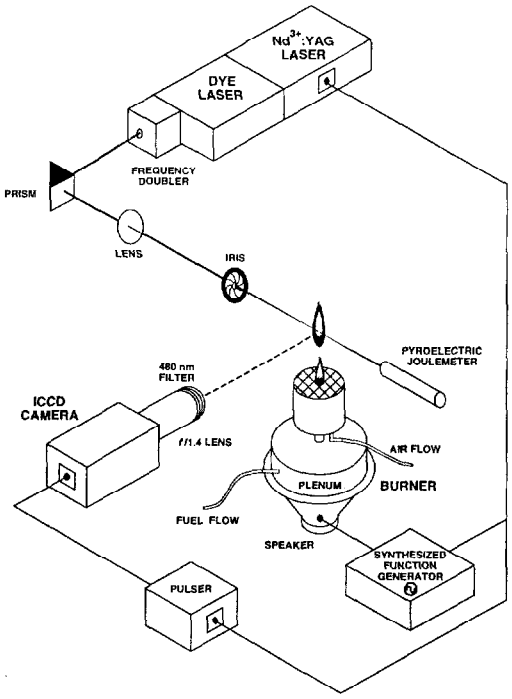

FIG. 1. Experimental set-up for 1-D imaging of axisymmetric diffusion flames which are acoustically excited and phase-locked to the pulsed dye laser system operating at 10 Hz. Images are recorded using an intensified charge-coupled device (ICCD) camera. The coannular burner is mounted on a vertical translation stage, allowing measurements to be performed from the burner lip up to a height of 115 mm.

Experimental Approach

Fluorescence imaging measurements of CO were made by exciting the Q branch (0,0) band of the $B^1\Sigma^+ \leftarrow\leftarrow X^1\Sigma^+$ transition with linearly polarized light near 230 nm in a two-photon process, and detecting fluorescence from the $B^1\Sigma^+ \rightarrow A^1\Pi$ (0,1) band at 483.5 nm. This excitation and detection scheme has been implemented for flame measurements by only four groups of researchers [8–13], despite the fact that excellent sensitivity can be obtained under favorable circumstances. The present application is the first in flames containing appreciable soot concentrations.

Figure 1 shows a schematic diagram of the burner and phase-locked imaging setup, which have been described in detail previously [1,2,14]. Unconfined laminar diffusion flames were stabilized on a coannular burner with a 10.2-cm diameter air annulus surrounding a 1.1-cm diameter fuel tube, with a loudspeaker attached to the plenum below the fuel tube. Experimental conditions were identical to those of our prior measurements in axisymmetric flames [1,2,14]. The mean cold flow velocities for the methane fuel and the air coflow were 7.8 cm/s and 7.9 cm/s, respectively, for both the steady and flickering flames, giving a visible steady flame height of 79 mm. OH· concentrations have been previously measured in this steady CH_4 flame [15], and the soot properties have been extensively investigated as well [1,2].

Laser-induced fluorescence measurements of CO were performed in the steady methane flame and in both moderately and strongly flickering flames produced by applying sine waves of magnitude 0.75 V and 1.5 V (peak-to-peak voltage), respectively, to the plenum loudspeaker. As with previous studies [1,2,14], the optical diagnostics were phase-locked to a sinusoidal oscillation of the fuel stream at the 10-Hz repetition rate of a Nd^{3+}:YAG laser, permitting phase-specific measurements in the time-varying flow fields. This frequency is close to the natural flame flicker frequency caused by buoyancy-induced instabilities (~12 Hz [14]). A synthesized function generator provided exact reproducibility of the flickering flame forcing amplitude and the detection phase settings. Figure 2 illustrates one complete cycle of OH· fluorescence and scattering images for the moderately flickering condition [14].

Line images of CO fluorescence were obtained at axial locations spaced every 5 mm. The incoming light at ~ 230 nm was generated by frequency-doubling the output of the Nd^{3+}:YAG-pumped dye laser using a beta barium borate crystal. With a linewidth of ~ 0.07 cm^{-1}, a pulse duration of ~4 ns, and energies of 0.8–1.3 mJ/pulse, this UV beam was focused at the burner centerline to a diameter of 440 μm (FWHM) using a 500-mm focal length lens. Fluorescence signals were recorded at 90° to the direction of the laser beam propagation on an intensified CCD camera using a narrowband dielectric filter with a bandpass of 480.0 ± 4.8 nm. For optimum detection sensitivity, an f/1.4 collection lens was employed with 4.4:1 imaging optics. The data were taken unbinned with a pixel resolution of 101 μm using 50-shot averages. To obtain line images, five rows were summed and binned by two in the radial direction, the background was subtracted, and the profile was normalized by the laser energy (see later).

Diagnostic Issues

Although methane is a lightly sooting fuel, the maximum soot volume fraction f_v reaches a level of 1.5–2.0 × 10^{-6} (ppm) in the clipped portions of the flickering flames. Severe interferences are observed upon excitation with ultraviolet light from these soot concentrations and the associated molecular precursors of soot. Diagnostic issues of interest are described next.

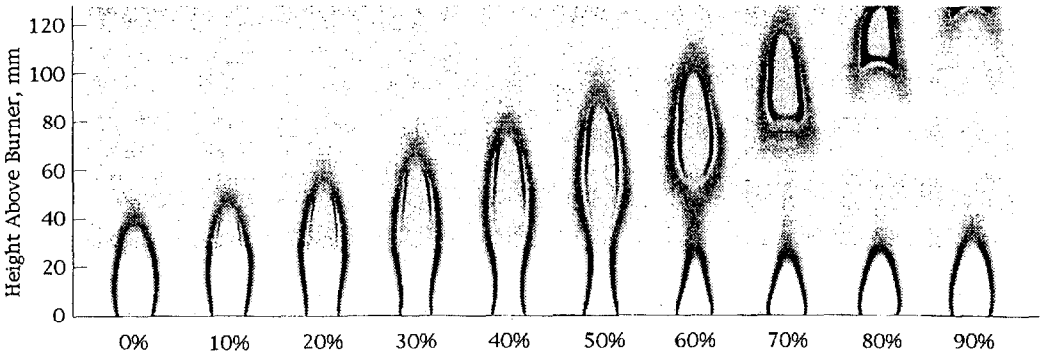

FIG. 2. Laser-energy-corrected OH· laser-induced fluorescence and soot scattering images in the time-varying laminar CH_4/air diffusion flame using horizontally polarized light at 283.55 nm [1]. A 0.75-V loudspeaker excitation is employed to give moderately flickering conditions. Ten phase increments separated by 10 ms are shown with an arbitrary zero phase.

Interferences

The laser intensities required for two-photon excitation of the CO $B^1\Sigma^+ \leftarrow\leftarrow X^1\Sigma^+$ transition (1–2 $\times 10^8$ W/cm^2) also lead to broadband laser-induced incandescence (LII) from soot particles [1,2], broadband fluorescence due to large molecular species (attributed to polycyclic aromatic hydrocarbons, PAH) [12,16], and laser-induced production of C_2 Swan band emission [8,16]. In order to minimize these interferences, profile measurements were made using narrowband detection. The dielectric filter centered at 480.0 nm effectively blocked the C_2 (1,0) Swan band emission (bandhead at 473.7 nm, blue degraded) but did pass some broadband emission from soot incandescence and molecular fluorescence. These broadband signals were often significantly stronger than the CO fluorescence, necessitating the subtraction of profiles measured with off-resonance excitation (at 230.08 nm). The interfering signals also exhibit different power dependences [2,17], which necessitates close attention to the beam intensity. The best net CO profiles were obtained when the on- and off-resonance measurements were made with the same laser intensity. In addition, the camera detector gate was set at its minimum width (18 ns) and was closed coincident with the end of the laser pulse in order to reduce the LII soot signal, which can exhibit decay times of 100–500 ns [18].

Selection of Rotational Line for Excitation

Since CO is rapidly oxidized in the high-temperature reaction zone (T_{max} = 2060 K in this flame [19]), significant CO levels occur only in rich flame regions over a relatively narrow temperature range. Prior measurements in steady CH_4/air diffusion flames have shown that appreciable CO exists only for T = 1500–2100 K [4,6,20]. No temperature measurements have been made for the flickering flames, but the modeling study of Kaplan et al. [5] indicates that temperatures in the rich regions are very similar to those in steady flame conditions. Selection of the best rotational line for CO imaging measurements involves a trade-off between fluorescence signal strength and the temperature dependence of the chosen rotational level. Modeling of the Q-branch rotational spectrum [11] reveals that the $J'' = 30$ and 32 levels are the least sensitive to temperature variations over the 1500–2100 K region in terms of number density and mole fraction imaging, respectively.

Figure 3 presents an excitation spectrum for CO $B^1\Sigma^+ \rightarrow A^1\Pi$ fluorescence obtained in a CH_4/air diffusion flame burning on a Wolfhard-Parker slot burner. Different detection filters and excitation wavelengths were tested using this burner, since its rectilinear geometry makes it ideally suited for fluorescence measurements. The spectrum shown in Fig. 3 was obtained low in the flame ($H \sim 4$ mm), where soot concentrations are negligible and molecular interferences are small. The $J'' = 30$ and 32 rotational lines can be distinguished in the excitation spectrum, but their fluorescence signals are relatively weak. Profile measurements were carried out using $J'' = 20$ to improve the overall signal-to-noise of the net CO profiles. For this selection of J'', the CO concentrations are overestimated for low temperatures and underestimated at high temperatures when calibrating the CO concentration at 1800 K (see later). The mole fraction errors are +35% at 1500 K and −24% at 2100 K, while the number density errors are +12% at 1500 K and −12% at 2100 K.

It is also of interest to compare area-integrated CO concentrations at a series of axial locations in the steady and flickering flames. This integration was performed by revolving the line profiles about the axis of symmetry. In order to estimate errors involved when the temperature field is not known (as

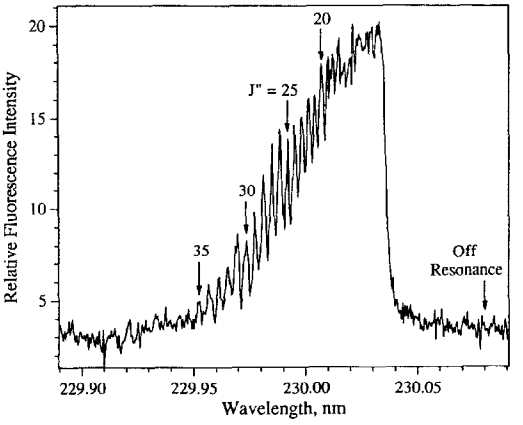

FIG. 3. CO fluorescence excitation spectrum for the Q-branch (0,0) band of the $B^1\Sigma^+ \leftarrow\leftarrow X^1\Sigma^+$ transition obtained with linearly polarized light in a two-photon process. Fluorescence from the $B^1\Sigma^+ \rightarrow A^1\Pi$ (0,1) band was detected with a dielectric filter/photomultiplier tube combination at 480.0 ± 4.8 nm. The spectrum was taken at $T \sim 1200$ K in a CH_4/air diffusion flame burning on a Wolfhard-Parker burner. Some distortion of the Q-branch bandhead occurs due to the transmission characteristics of the detection filter (see text). Low J levels are not resolved due to collisional broadening; higher rotational lines have been assigned by comparison with computed spectra [11].

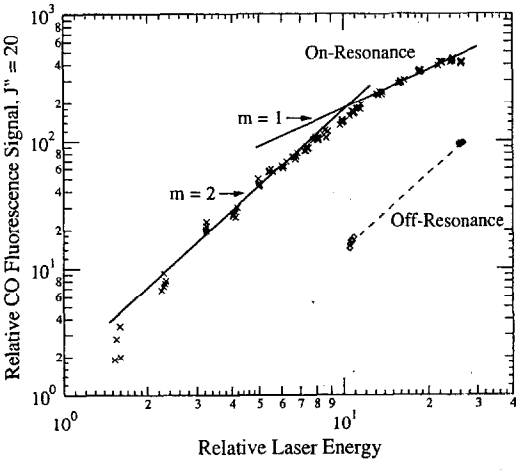

FIG. 4. CO fluorescence signal as a function of laser energy for on-resonance excitation (crosses; $J'' = 20$) and off-resonance excitation (diamonds); see also Fig. 3.

in the flickering flames), results were compared at H = 30 mm in the steady flame with and without a temperature correction. The concentration errors in the line profiles at low and high temperatures are largely off-setting for the area integrations, giving an overall error of +4.3% for the CO mole fraction and +1.8% for the CO number density. Volume integrals were obtained by summing the area integrals at all axial locations for the steady flame and each phase of the flickering flames.

Intensity Dependence and Quenching

For two-photon excitation of the CO $B^1\Sigma^+ \leftarrow\leftarrow X^1\Sigma^+$ transition, the fluorescence signal S is expected to be proportional to the square of the laser intensity I at low intensities [11]:

$$S \propto N_1 W_{12}/(Q + A + P + \sigma I)$$

Here, N_1 is the Boltzmann population of the ground state rotational level excited, W_{12} is the rate coefficient for two-photon absorption from the ground electronic state ($\propto I^2$), and Q, A, P, and σI are the total rates for quenching, radiative decay, predissociation, and photoionization from the excited electronic state, respectively. Radiation and predissociation rates are much smaller than quenching rates for the present conditions [11]. An I^2 intensity dependence is not observed, however, since the excitation rate to the $B^1\Sigma^+$ state is small. Fluorescence signals are detected in flames only for sufficiently large laser intensities that the ionization rate always competes with quenching. At high intensities, when $\sigma I \gg Q$, the fluorescence signal becomes linear with laser intensity and independent of the local quenching rate, which varies considerably as a function of position in a diffusion flame. Therefore, operation at high laser intensities has advantages for CO imaging measurements beyond improved signal strengths: (1) no quenching corrections are required, and (2) the linear CO fluorescence signals can be easily corrected for laser intensity variations on a shot-to-shot basis.

Figure 4 presents the measured CO fluorescence signal as a function of laser energy at a flame location where soot is not present and broadband fluorescence from molecular species is weak. These data were obtained using the intensified CCD camera and exhibit a linear dependence for higher energies, as found in prior investigations [9–11]. At the highest energies, the fluorescence signal is essentially independent of laser energy, most likely due to ionization depletion of CO in the focal volume.

Dispersed fluorescence scans revealed that the emission wavelength varied with the rotational line excited. This observation verifies that the photoionization rate exceeds the quenching rate under our experimental conditions. Emission occurs predominantly from the rotational level initially excited when rotational energy redistribution is slow relative to photoionization. Since the rotational constants (B values) for the ground and excited electronic states differ, the CO fluorescence wavelength changes (by up to 5 nm) depending upon the rotational line initially excited. One can utilize this behavior to tune the fluorescence wavelength to best match the

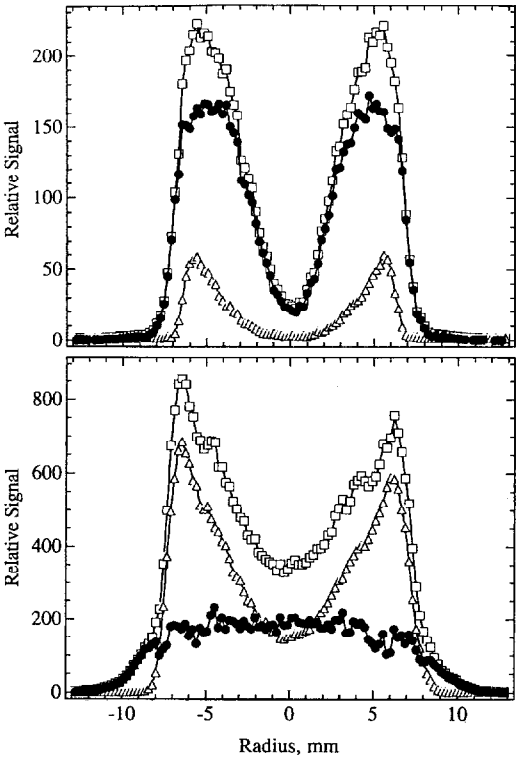

FIG. 5. CO profile results obtained in flame locations where background interference is small (top; steady flame at H = 5 mm) and large (bottom; moderately flickering flame at H = 70 mm for 60% phase; see Fig. 2). Note the different ordinate scales. In each case the on-resonance data (J'' = 20 at 230.007 nm; squares), off-resonance data (230.08 nm; triangles), and net profiles (filled circles) are presented for 50-shot averages. The laser beam propagates from left to right.

transmission band of a given detection filter by exciting an appropriate rotational line. Conversely, a particular narrowband dielectric filter will effectively transmit CO fluorescence only when exciting a limited number of rotational lines.

Calibration

The two-photon CO fluorescence signal was calibrated in three CH_4/air diffusion flames, wherein absolute CO concentrations and temperature profiles are available. These measurements include (1) infrared absorption using a tunable diode laser at H = 30 mm in the present axisymmetric flame [21], (2) mass spectrometric measurements at H = 80 mm in a taller methane flame (visible flame height = 107 mm [22]), and (3) tunable diode laser data at H = 9 mm in a Wolfhard-Parker burner flame [20]. The CO temperature-corrected fluorescence profiles measured in these flame/burner configurations were compared against the earlier results at their peak concentrations (3.1, 4.1, and 3.4 mole percent, respectively) and showed excellent agreement, with a standard deviation of ±3.7%. If additional data are considered, including mass spectrometric results in the Wolfhard-Parker flame [20,23], the uncertainty in this calibration procedure increases to ± 13%. The profile shapes of the present temperature-corrected line images are in reasonably good agreement with the measurements cited above [20–22].

Linewidth Considerations

The observed linewidth in the CO fluorescence spectra (Fig. 3) is typically ~0.65 cm^{-1}, which is considerably larger than the laser bandwidth of ~ 0.07 cm^{-1}. A variation in the CO linewidth with flame position could effect the profile results, since the two-photon absorptivity coefficient depends upon the centerline signal intensity for a narrow-line excitation source. However, no significant differences in CO rotational linewidths were observed for spectra measured at several lateral positions in the Wolfhard-Parker supported methane flame.

Corrections for Beam and Signal Attenuation

Absorption of either the incident laser beam at 230 nm or the fluorescence emission at 483 nm is negligible in the steady CH_4/air diffusion flame, since the concentrations of soot particles and large molecules are small (maximum f_v = 0.33 ppm [2]). However, beam and signal attenuation are expected to be at least five times greater for flickering flame conditions. Extinction measurements revealed that the attenuation of 230-nm light was as high as 20–25% in the clipped portions of the flickering flames, whereas it reached only 6% in the steady flame (at H = 40–50 mm). Attenuation of the incident radiation has two effects: (1) CO fluorescence signals are reduced; but (2) the derived net CO signals are too large, since the laser beam energy used to give an energy-corrected profile at each axial location was measured after the flame (see Fig. 1). In the regions of the flickering flames where beam attenuation is greatest, this overprediction of the CO concentration can be as much as 15%. The effect of beam attenuation upon the volume integral of the profiles obtained in the moderately flickering flame at 60% phase (see Fig. 2) is to overpredict the total CO concentration by 7%.

Extinction of the CO fluorescence signal arises mainly from the soot layer, since absorption by large molecules is much weaker in the visible region compared to the ultraviolet [16]. The effect of signal attenuation is to underestimate the actual CO concentrations. However, the estimated fluorescence extinction is only 4–5% in the flickering flames at

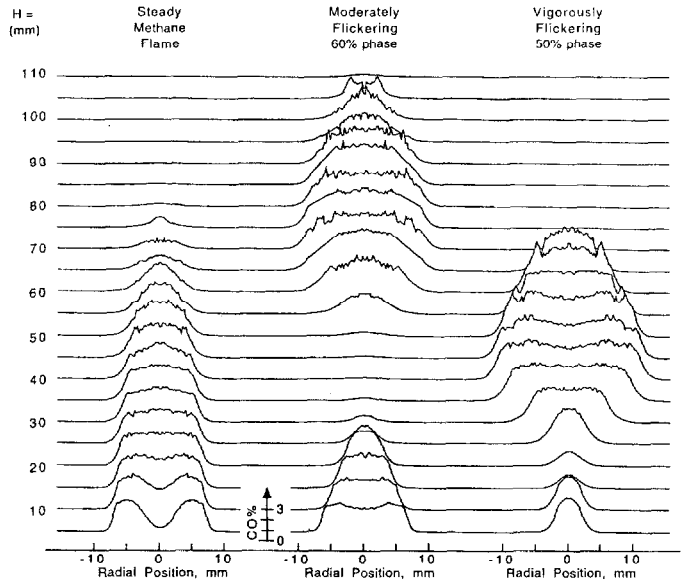

FIG. 6. Calibrated, laser-energy-corrected, net CO fluorescence profiles for the steady CH_4/air diffusion flame (left), the moderately flickering flame at 60% phase (middle; see Fig. 2), and the vigorously flickering flame at 50% phase (right).

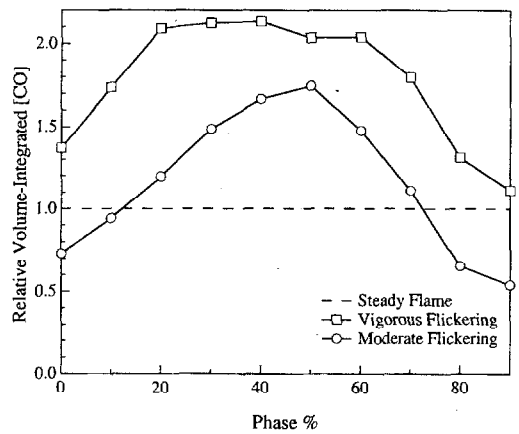

FIG. 7. Volume-integrated CO concentrations for the moderately flickering (circles) and vigorously flickering (squares) CH_4/air flames normalized by the steady flame volume integral, shown as a dotted line (see text).

maximum soot loading, and therefore this correction was not included in the data analysis.

Results and Discussion

Figure 5 presents typical profile results at flame locations where the interferences from broadband molecular fluorescence and soot incandescence are small (low in the steady flame) and large (in the clipped portion of the flickering flame). When the maximum soot volume fraction reaches 1–2 ppm in the flickering flames, the magnitude of the off-resonance signal approaches 70–80% of the on-resonance signal. Subtraction of the off-resonance profiles from the on-resonance data was often imperfect under these conditions, primarily due to flame instabilities coupled with the sharp annular structure of the soot field. For obtaining area-integrated CO concentrations, a representative straight line was drawn through the soot layer for these cases.

CO imaging measurements were also attempted for more heavily sooting ethylene flames, in which interferences from laser-induced soot incandescence and broadband fluorescence are severe. Only at low axial locations in the steady flame where $f_v \leq$ 5 ppm could CO concentration data be obtained. Here, the net CO profiles exhibited a smooth variation across the soot layer, as expected since soot oxidation rates are small at this location [24]. CO fluorescence measurements in flickering ethylene flames, where the soot volume fraction reaches 20 ppm [2], proved to be intractable.

Figure 6 compares CO concentration profiles for the steady methane flame and two phases of the flickering flames that illustrate tip clipping (see Fig. 2). The flickering CO profiles are broader following clip-off and extend to higher axial locations than in the steady flame. Maximum CO mole fractions are comparable in the steady and flickering flames: 3.0–4.0% for the steady and moderately flickering conditions and up to 5.3% for the vigorously flickering case, in agreement with recent tunable diode laser measurements of CO in the same flames [21].

Figure 7 presents the results of volume-integrating these CO profiles for each phase of the flickering flames, normalized to the steady flame integral. The greater radial extent of the clipped-off flamelets

yields larger volume-integrated CO levels for 6 out of 10 phases in the moderately flickering flame and all phases in the vigorously flickering flame. Unfortunately, the experimental set-up restricted the CO imaging to a maximum height of 115 mm above the burner, limiting the domain over which the volume integral could be computed for the flickering flames. In addition, some error is inherent in averaging over the limited temporal and axial sampling. The underestimation due to the measurement height constraint for the strongly flickering methane flame is relatively small, since this flame has a luminous height of ~ 130 mm and CO concentrations are low by $H = 115$ mm. For the moderately flickering flame, however, the luminous height is ~ 170 mm, resulting in approximately a 25% underestimation of the total CO concentration, based upon analysis of our soot measurements in the same flames [2]. When the volume-integral results are averaged over all times, the total CO concentration compared to the steady flame increases by ~50% in the moderately flickering flame (accounting for the 25% underestimation) and by ~65% in the vigorously flickering case. The variation in the integrated CO levels observed as a function of phase in Fig. 7 arises because the instantaneous flame size is largest at midcycle, whereas the clipped portion of the flame burns out (and therefore is smaller) at early and late phases (see Fig. 2).

Although soot concentrations increase dramatically in flickering methane flames compared to steady flame conditions (five to six times for the maximum soot concentration and four times when time-averaged and volume-integrated [1]), CO concentrations increase much more modestly. Methane is a lightly sooting fuel, such that soot oxidation has a relatively small impact upon local CO levels. For example, a flux calculation in the steady CH_4/air flame shows that only ~0.85% of the initial fuel carbon atoms are converted to soot particles at $H = 50$ mm above the burner, where the peak soot volume fraction occurs [1]. In contrast, the corresponding CO profile accounts for ~7.3% of the fuel carbon. Thus, for the higher soot loadings measured in the flickering flames, complete oxidation of soot to CO would not even double the total CO concentration. Similarly, neither the competition between soot particles and CO for the available OH· in the oxidation region of the flickering flames nor the increased radiation losses in the flickering flames appear to have a significant influence on CO concentrations. However, in more heavily sooting flames, all of these factors may have a greater impact. Puri and Santoro [4,6] have measured increased centerline CO concentrations for increased soot loadings in the oxidation region of a series of methane, methane/butane, and methane/butene flames. Skaggs and Miller reported similar results in a series of ethylene diffusion flames [25]. Furthermore, nonsmoking, steady propane and ethylene flames are observed to readily emit smoke for flickering flame conditions [2]. Therefore, the increased total CO levels created in flickering flames will lead to greater CO emission for hydrocarbon fuels that emit smoke under flickering flame conditions.

Conclusions

One-dimensional, two-photon CO imaging measurements are tractable in sooting, hydrocarbon diffusion flames so long as the peak soot volume fraction, f_v, does not exceed 5 ppm. At higher soot loadings, interference from both laser-induced soot incandescence and broadband fluorescence from large molecular species becomes much stronger (more than 20 times) than the CO fluorescence signals.

Flickering CH_4/air diffusion flames exhibit time-averaged, volume-integrated CO concentrations ~50–65% larger than a steady flame burning with the same mean fuel flow rate. This enhanced CO production is small compared to the fourfold increase in the time-averaged, volume-integrated soot concentration [1], suggesting that soot oxidation does not have a major impact on CO levels for flames where $f_{v,max} \leq 1$–2 ppm. Furthermore, maximum CO concentrations are approximately equal in the steady and flickering flames; no evidence of localized high CO concentrations was obtained under flickering conditions.

Acknowledgment

We thank the Basic Research Group of the Gas Research Institute for their partial support of the this work under Contract 5093-260-2676.

REFERENCES

1. Shaddix, C. R., Harrington, J. E., and Smyth, K. C., *Combust. Flame* 99:723–732 (1994) and 100:518 (1995).
2. Shaddix, C. R. and Smyth, K. C., *Combust. Flame,* in press.
3. Roth, P., Brandt, O., and Von Gersum, S., *Twenty-Third Symposium (International) on Combustion,* The Combustion Institute, Pittsburgh, 1990, p. 1485.
4. Puri, R., Santoro, R. J., and Smyth, K. C., *Combust. Flame* 97:125–144 (1994), and Erratum *Combust. Flame* 102:226–228 (1995).
5. Kaplan, C. R., Shaddix, C. R., and Smyth, K. C., *Combust. Flame,* 106:392–405 (1996).
6. Puri, R. and Santoro, R. J., *Fire Safety Science: Proceedings of the Third International Symposium,* Elsevier Applied Science, London and New York, 1991, pp. 595–604.

7. Turns, S. R. and Bandaru, R. V., *Combust. Flame* 94:462–468 (1993) and references therein.
8. Aldén, M., Wallin, S., and Wendt, W., *Appl. Phys. B* 33:205–212 (1984).
9. Haumann, J., Seitzman, J. M., and Hanson, R. K., *Opt. Lett.* 11:776–778 (1986).
10. Seitzman, J. M., Haumann, J., and Hanson, R. K., *Appl. Opt.* 26:2892–2899 (1987).
11. Tjossem, P. J. H. and Smyth, K. C., *J. Chem. Phys.* 91:2041–2048 (1989).
12. Smyth, K. C. and Tjossem, P. J. H., *Appl. Opt.* 29:4891–4898 (1990).
13. Fiechtner, G. J., Barlow, R. S., and Carter, C. D., in preparation.
14. Smyth, K. C., Harrington, J. E., Johnsson, E. L., and Pitts, W. M., *Combust. Flame* 95:229–239 (1993).
15. Puri, R., Moser, M., Santoro, R. J., and Smyth, K. C., *Twenty-Fourth Symposium (International) on Combustion*, The Combustion Institute, Pittsburgh, 1992, p. 1015.
16. Smyth, K. C., Miller, J. H., Dorfman, R. C., Mallard, W. G., and Santoro, R. J., *Combust. Flame* 62:157–181 (1985).
17. Harrington, J. E., Shaddix, C. R., and Smyth, K. C., *SPIE International Symposium on Laser Diagnostics in Combustion*, Society of Photo-Optical Instrumentation Engineers, Bellingham, WA, 1994, Vol. 2124, Paper 20.
18. Quay, B., Lee, T.-W., Ni, T., and Santoro, R. J., *Combust. Flame* 97:384–392 (1994).
19. Richardson, T. F. and Santoro, R. J., personal communication, 1993.
20. Miller, J. H., Elreedy, S., Ahvazi, B., Woldu, F., and Hassanzadeh, P., *Appl. Opt.* 32:6082–6089 (1993).
21. Skaggs, R. R. and Miller, J. H., *Technical Meeting of the Eastern States Section of the Combustion Institute*, Clearwater FL, 1994, pp. 172–175; see also this symposium.
22. Puri, R. and Santoro, R. J., personal communication, 1993; see also Ref. 4.
23. Norton, T. S., Smyth, K. C., Miller, J. H., and Smooke, M. D., *Combust. Sci. Technol.* 90:1–34 (1993).
24. Santoro, R. J., Yeh, T. T., Horvath, J. J., and Semerjian, H. G., *Combust. Sci. Technol.* 53:89–115 (1987).
25. Skaggs, R. R. and Miller, J. H., *Combust. Flame* 100:430–439 (1995).

COMMENTS

Robert S. Barlow, Sandia National Laboratories, USA. Are there plans to use the thin-filament temperature measurements reported in Pitts [1] to correct the present CO measurements?

Unpublished measurements and analysis by Greg Fiechtner at Sandia National Labs have shown that it is possible to have a sublinear power dependence of the CO fluorescence signal, and consequently, a measured power dependence of unity at a particular laser energy does not guarantee quenching independence. This effect may not be important for the present measurements, but it is important, in general, to consider these details of the CO LIF power dependence.

REFERENCE

1. Pitts, W. M., *Twenty-Sixth (International) Symposium on Combustion*, The Combustion Institute, Pittsburgh, 1996, pp. 1171–1179.

Author's Reply. One of the goals of the present investigation was to make quantitative CO measurements under conditions where the detailed temperature field was unknown, i.e., in the flickering flames. However, appreciable CO concentrations are expected to exist only for temperatures in the 1500–2100 K range, and on this basis we calculated our maximum expected errors. When the subsequent thin-filament temperatures measurements of Pitts became available, we compared our integrated CO concentration for one phase of the moderately flickering flame (60%) with that determined using "temperature-corrected" profiles. For this case our analysis gives an integrated CO mole fraction 6.9% higher than when including the thin-filament temperatures, consistent with our error estimates. Further analysis is not warranted until the filament temperatures can be corrected for heat losses due to radiation.

We certainly agree that all contributions to the CO fluorescence power dependence should be examined carefully. Briefly mentioned in the text is additional evidence that the present CO measurements were carried out under quenching-independent conditions. When the laser intensity was sufficiently high to observe a linear power dependence, spectral scans of the fluorescence emission exhibited a shift in wavelength which depended upon the rotational line excited. This change in wavelength was precisely that expected for emission dominated by a single rotational line. Thus, under our experimental conditions the photoionization rate was much faster than rotational energy transfer (and likely collisional quenching as well) in the B state of CO. In addition, our estimated ionization rate from the B state ($>10^{10}$ s^{-1}; see also [11]) is expected to be considerably higher than the quenching rate. Recently a value of $2.5–4.0 \times 10^9$ s^{-1} has been measured for quenching of the CO B state in a premixed methane/oxygen flame [1].

REFERENCE

1. Agrup, S. and Aldén, M., *Appl. Spectr.* 48:1118–1124 (1994).

A. Morhov, N.V. Nederlandse Gasunie, Netherlands. The two-photon LIF of carbon monoxide is a function of the flame temperature and CO concentration. If the measurements are performed in a point where the temperature and CO concentration fluctuate and these fluctuations are correlated then the derived average CO concentration can be biased to real average value. What is the magnitude of the bias in your measurements?

Author's Reply. The bias you describe should be negligible in these flames, because they are laminar and the acoustic forcing of the methane flow velocity renders the flickering flame behavior highly reproducible. Although we typically average 50 laser shots for the data reported here, our prior soot measurements [1, 2, 14] indicate that the profiles are nearly identical for each individual shot.